Reactivity of Au nanoparticles supported over SiO_2 and TiO_2 studied by ambient pressure photoelectron spectroscopy

Tirma Herranz[1], Xingyi Deng[1], Andreu Cabot[1], Paul Alivisatos[1], Zhi Liu[2], Galo Soler-Illia[3] and Miquel Salmeron[1,4]

[1]Materials Sciences Division and [2]Advance Light Source, Lawrence Berkeley National Laboratory; [3]Unidad de Actividad Química, Comisión Nacional de Energía Atómica UAQ-CAC-CNEA, Buenos Aires, Argentina; [4]Materials Science and Engineering Department, University of California, Berkeley

Keywords: Gold, titanium oxide, ambient pressure photoelectron spectroscopy, in situ XPS, model catalysts.

Abstract

The influence of the metal cluster size and the identity of the support on the reactivity of gold based catalysts have been studied in the CO oxidation reaction. To overcome the structural complexity of the supported catalysts, gold nanoparticles synthesized from colloidal chemistry with precisely controlled size have been used. Those particles were supported over SiO_2 and TiO_2 and their catalytic activity was measured in a flow reactor. The reaction rate was dependent on the particle size and the support, suggesting two reaction pathways in the CO oxidation reaction. In parallel, ambient pressure photoelectron spectroscopy (APPS) has been performed under reaction conditions using bidimensional model catalysts prepared upon supporting the Au nanoparticles over planar polycrystalline SiO_2 and TiO_2 thin films by means of the Langmuir-Blodgett

(LB) technique to mimic the characteristic of the powder samples. In this way, the catalytically active surface was characterized under *true* reaction conditions, revealing that during CO oxidation gold remains in the metallic state.

1. Introduction

Bulk gold is known for its inertness in chemical reactions [1]. Nevertheless, in the late 1980, Haruta discovered that gold nanoparticles dispersed in an oxide support are active for the low temperature CO oxidation [2]. Since then, an increasing number of reports dealing with many different reactions catalyzed by supported gold catalysts have followed [3,4]. Investigations using *in-situ* characterization of supported gold catalysts under reaction conditions are, however, in an early stage. Most of these studies deal with the CO oxidation because of its potential for practical applications, like the purification of H_2 streams by preferential oxidation of CO (PROX) in order to avoid the deactivation of Pt in fuel cell related catalysts. Supported gold nanoparticles are extremely active in this reaction at temperatures as low as 200 K [5]. The effect of the Au particle size was first studied by Haruta *et al.* with supported catalysts, showing that the Au cluster size is a key factor for the catalytic activity [6]. It is now well established that the size of the gold nanoparticles must be below 5 nm in order to obtain an active catalyst [7]. It is not clear yet if the particle size is a primary variable affecting the activity or if the particle morphology or structure of the metal-support interface is the key parameter [8]. Some authors have pointed out that the support plays an important role in the CO oxidation reaction and that more active catalysts are obtained when the gold clusters are deposited on reducible oxides, especially TiO_2 [4,9,10]. By contrast, Norskøv *et al.* have suggested that the support does not play any role in the CO

oxidation reaction. The low coordinated gold atoms are responsible for the catalytic activity instead [11].

Furthermore, different proposals can be found on the literature about the nature of the active site(s) responsible for the CO oxidation in supported gold catalysts. The high reaction rate has been attributed to either metallic gold atoms at the Au-support interface [12] and/or to low coordinated atoms in the gold clusters [13]. Bond and Thompson [14] have suggested that the active sites are gold ensembles incorporating metallic and cationic (3+) gold atoms, the latter located at the metal-support interface. It has been proposed that metallic [15], cationic [16], and even anionic gold species [17] could be the active sites responsible for the high activity observed with Au catalysts in CO oxidation.

The typical supported gold catalyst consists of Au nanoparticles of different sizes and shapes dispersed on an amorphous support, usually a high area metal oxide powder. There have been some attempts to overcome the inherent structural complexity of supported catalysts by preparing "model samples". These models consist of planar support surfaces (usually a single crystal) [3,18] with gold clusters deposited on top. On these samples, surface characterization techniques operating in ultrahigh vacuum can be used. These systems have the limitation of lacking some important characteristics of potential practical catalysts, such as support hydroxyl groups and/or water. The use of clusters of gold with selected sizes provides a way to control on of the variables of the system [19]. In this work, we used gold clusters with a narrow size distribution and polycrystalline flat supports which mimic the characteristic of powder ones, such as the high area or the presence of surface hydroxyl groups. Moreover, we use a novel *in situ* technique, ambient pressure photoelectron spectroscopy (APPS), capable of providing

spectroscopic information on the chemical state of the surface and the influence of reactant gases during reaction conditions.

2. Experimental

Colloidal gold nanoparticles with sizes in the range between 2 and 5.5 nm were synthesized by the reduction of gold (III) chloride hydrate (99.999%) with tetrabutyl ammonium borohydride (TBAB, 98%) in the presence of didodecyldimethylammonium bromide (DDAB, 98%) and dodecylamine (99%), as previously described by Jana *et al.* [20]. In a typical synthesis, 0.1mmols of $HAuCl_4$ were dissolved in 10 ml of a 0.1M DDAB solution in toluene. Next, 1 mmol of dodecylamine was added to the solution and dissolved by sonication. Finally, a solution of 0.3 mmol TBAB dissolved in 2 ml of 0.1M DDAB in toluene was rapidly injected into the gold chloride solution under vigorous stirring. As a product of this reaction, 2-3 nm gold nanoparticles were obtained. Larger particles, up to 5 nm, were obtained by seeded growth from this initial sample. Gold nanoparticles were grown by introduction of an additional gold precursor, which was slowly reduced using a hydrazine solution. Following the synthesis process, the samples were cleaned several times by means of precipitation with alcohols and re-dispersion in chloroform. After the synthesis, 0.5 mmol hexadecanethiol were added to the nanoparticle solution to prevent aggregation. The synthetic route allowed the preparation of gold nanoparticles with size distributions around 10%. Figure 1 shows a typical TEM micrograph of 4.8±0.4 nm Au particles and the corresponding histogram of the particle size distribution. The other samples (with different Au cluster size) display Au particles of similar shape and narrow distribution.

For CO oxidation experiments gold nanoparticles dispersed in chloroform were supported on high area commercial SiO_2 (Cab-O-Sil H-5 Cabot Corporation, 300 m^2/g) or TiO_2 (Degussa P25, 42 m^2/g). The method used for dispersing the particles in the

support has been previously described [21]. Briefly, the support and the nanoparticles were mixed in an aprotic solvent, specifically chloroform, and sonicated for 60 min. Next, the mixture was filtered and dried in an oven at 80ºC for 16 h. The samples were characterized before and after reaction by X-ray photoelectron spectroscopy, XPS (PHI 5400) and transmission electron microscopy (JEOL 2100-F 200 kV). In this instrument it is possible to perform high resolution transmission electron microscopy (HRTEM) and high-angle annular dark field (HAADF) scanning transmission electron microscopy. The intensity of the electrons collected in the last technique is approximately proportional to Z^2, allowing z-contrast imaging.

The catalytic activity was measured in a U-shaped quartz reactor. The reactor was placed in an oven connected to a PID temperature controller (Watlow). The gas flow was regulated by mass flow controllers (Porter Instruments). Before measuring the catalytic activity, the hexadecanethiol molecules protecting the Au clusters were removed by submitting the sample to a temperature-programmed treatment in O_2/Ar (10vol.%) at 300ºC (heating rate 5ºC/min) and dwell time of 60 minutes. After the pretreatment, the samples were cooled down in O_2/Ar and the rate of carbon monoxide oxidation was measured at increasing temperatures (from 20 to 100ºC) and 0.1 MPa of total pressure. The gas flow rate was 40 ml/min (5 CO/5O_2/20Ar). The evolution of the concentration of the different compounds was monitored by selected m/z fragments that were analyzed by means of a quadrupolar mass spectrometer connected on line to the reactor outlet.

For spectroscopy studies we have used films of Au nanoparticles deposited on a flat substrate by the Langmuir-Blodgett (LB) method [22,23]. The substrate was either SiO_2/Si wafers (native oxide layer over a silicon wafer) or nanoporous TiO_2 films over a Si wafer [24 , 25]. Before the spectroscopic measurements, the samples were

characterized by scanning electron microscopy (Zeiss Gemini Ultra-55 Analytical Scanning Electron Microscope) and XPS (described above). To remove the thiols, the samples were cleaned with an UV/ozone cleaner during 60 min.

Ambient pressure photoemission spectroscopy (APPS) experiments were performed using a spectrometer capable of operating at ambient pressures in the Torr range at the beamline 9.3.2 at the Advanced Light Source (Berkeley, USA) [26 , 27]. The spectrometer consists in a chamber with a differentially pumped electrostatic lens system that focuses the electrons emitted by the sample into the focal plane of a hemispherical electron energy analyzer.

The catalytic activity of Au for CO oxidation with O_2 could be monitored using a mass spectrometer connected to the second pumping stage of the instrument, just before the analyzer. Photoemission spectra of the Au4f, C1s, Ti2p, O1s, Si2p, core levels were recorded using photon energies of 400 eV (Au and Si), 600 eV (C), 720 eV (Ti) and 850 (O) eV, respectively, which produce photoelectron emitted approximately the same kinetic energy (300-350 eV), thus, ensuring the same analysis depth. The binding energy scale in all experiments was calibrated using the known value Ti3p (37.5 eV) as a reference [28]. A Shirley background was substrated from all spectra before deconvolution. The peaks were fitted using Gaussian-Lorentzian curves. The separation between the spin-orbit coupled peaks Au $4f_{7/2}$ and Au $4f_{5/2}$ was found to be 3.67 eV with a branching ratio of 4:3. The area of the peaks has been normalized by the incident photon flux.

3. Results and discussion

3.1. Powder samples characterization

Figure 2 shows selected TEM and HRTEM micrographs of gold nanoparticles supported on silicon oxide and titanium dioxide. On SiO_2 the nanoparticles were randomly distributed. Their shape is mainly spherical although some faceted particles having hexagonal shape can be seen. Conversely, gold nanoparticles were found at the edges of the anatase phase when supported on TiO_2-P25 (evidence by electron diffraction). In all cases, the gold nanoparticles are single crystal metallic Au (face centered cubic, fcc). The large difference in atomic number between the gold (Z=79) and the oxide supports (oxygen, 8, silicon, 14, and titanium, 22) allows detection of the nanoparticles with high contrast using the STEM-HAADF detector as it is very sensitive to the atomic weight (Figure 3). In the Au/SiO_2 samples the spatial distribution of Au particles is random, with no preferential location. On the other hand, when TiO_2 is used, the gold nanoparticles are evenly distributed over the support and located at the edges of the titania particles.

X-ray photoelectron spectroscopy of the as-prepared samples (Figure 4a) shows that the gold atoms are in the metallic state on both supports (SiO_2 and TiO_2). There is only one peak in the $Au4f_{7/2}$ region, located at 83.8 eV (metallic gold). It can not be discarded the presence of an extra peak at higher binding energies, although the low signal to noise ratio makes the assignment difficult.

3.2. Catalytic activity

The thiols covering the gold nanoparticles were removed before testing the catalytic activity of the samples. This was performed by heating the samples in diluted oxygen (10% O_2/Ar) at 5ºC/min from room temperature to 300ºC, and then keeping this temperature for 60 minutes [21]. During the thermal treatment the effluent gases were analyzed by mass spectroscopy. Water was first detected at 80-110ºC. Next, CO_2

(formed by decomposition of the hydrocarbon chains of the surfactants) was detected at 150°C and 300°C. To test if the heating treatment was sufficient to optimize the nanoparticles reactivity, the specific activity of the 2 nm sample for CO oxidation at 70°C was recorded as a function of the treatment temperature from 120 to 500°C (Figure 5). The specific activity increases linearly with the temperature until 200°C. From this point, on further increases in the treatment temperature do not affect the reaction rate, with the activity remaining stable even when the sample was treated at 500°C.

The first parameter investigated in the reactivity of the gold nanoparticles was the effect of the support. We chose the 3.7 nm sample and test the catalytic activity for CO oxidation after the treatment in O_2/Ar at 300°C. At shown in Figure 6a, below 50°C the specific activity of the gold nanoparticles is similar on both supports. When the temperature increases, the activity in the case of the silica support remains flat and even decreases. In contrast, on the titania support the activity rises rapidly with temperature. At 90°C its activity is about 7 times higher on TiO_2 than on SiO_2. These results clearly indicate that there is an effect of the oxide support in the reactivity of gold catalysts, at least at the higher temperatures, consistent with the results published by Arrii *et al.* [9]. In our experiment, the gold nanoparticles come from the same batch, and therefore, there are no other external factors that could affect their reactivity. This is not the case for samples prepared by deposition-precipitation, which can lead to the formation of nanoparticles with different shapes and sizes depending on the surface composition and morphology of the substrate.

Using the titania support, the effect of the particle size (2-6 nm range) was evaluated in the CO oxidation reaction at 70°C (Figure 6b). When the particle size decreases, the specific activity (per gram of gold) increases dramatically, in agreement with most of the published data on supported gold [29,30,31]. We did not observe however, the

volcano plot (specific activity *vs.* cluster size) described by Goodman *et al.* [18] who could use much smaller gold clusters (up to 1 nm in size and 2 monolayer thickness). Therefore, our data do no preclude the existence of a peak in reactivity at a size below 2 nm.

After reaction, the samples were characterized again by XPS and TEM. The XPS data showed that in the Au 4f region there is only one peak at 83.8 eV in all the samples, indicating that after reaction the gold nanoparticles remain in the metallic state. Figure 7 displays TEM and HRTEM micrographs of selected used samples supported over SiO_2 and TiO_2. There is some agglomeration on the samples supported over silica, especially for the 2 nm gold particles. This agglomeration is more pronounced in the case of samples supported over titania, where particles showing different domains can be distinguished in the 2 nm sample. The reason why the gold particles on TiO_2 show a higher degree of agglomeration might be due to the low surface area compared with the silica (42 and 300 m^2/g). Despite of this fact, the activity over TiO_2 is still higher than on silica. It is important to remark that in these samples the facetted particles have become spherical in shape.

At temperatures above 50ºC the gold nanoparticles display an activity that is clearly higher when supported on TiO_2, in agreement with the theories proposing than the support has a strong influence in the catalytic performance. Liu *et al.* using DFT calculations [32] proposed that CO oxidation occurs at the interface between gold and the titanium dioxide being the oxygen activation the rate determining step. Bulk gold (single crystal or polycrystalline) does not adsorb molecular oxygen, only small Au particles can do it. The CO, however, can be adsorbed on the surface as demonstrated theoretically and experimentally [33,34]. Therefore, it is necessary to activate the O_2 molecule to initiate the CO oxidation [35]. The interaction between the gold

nanoparticles and adsorbed oxygen is thought to be produced by electron donation and back donation between the orbitals 6s and 6p of the Au and the π^* orbital of the oxygen molecule that weakens the O-O bond. The promoting effect of the support oxide could consist in the enhancement of this electron transfer [32]. This is in line with theoretical studies that propose that molecular oxygen can adsorb forming a peroxo species onto gold clusters. This chemisorption can also cause a change in the shape of the cluster [36].

The effect of the particle size is also evident in the present study. When the size decreases, the specific activity is higher. Many authors propose that the key factor of the activity in Au catalysts is the presence of under-coordinated gold atoms [37,38] which adsorb CO and oxygen more strongly, making the reaction possible.

The fact that both the support and the particle size influences on the reaction rate is in agree with theories proposing the existence of several reaction pathways occurring simultaneously with reducible supports [39,40]. One pathway implies only the gold nanoparticles, being the particle size critical, as smaller particles have a higher number of under-coordinated sites. The other pathway involves the participation of the support, where the oxygen can be activated more easily, either on the support itself or in the gold-support perimeter. This last reaction pathway has found to be more important when the temperature increases, maybe because the adsorption of oxygen on gold nanoparticles is weaker at high temperatures. On silicon oxide, as non reducible support, only the first mechanism operates, explaining its less activity at high temperatures.

3.3. Planar model catalysts preparation and characterization

Selected gold nanoparticles with 2 and 3.7 nm sharp size distribution were deposited on titania and silica thin films using the Langmuir-Blodgett technique. In order to remove

the surfactant and thiols, the samples were cleaned with ozone. Figure 8 shows high resolution scanning electron micrographs of the samples after cleaning. The gold nanoparticles are spread over the support with a loading of 0.4-0.7 monolayer and even after the cleaning treatment they keep their shape and size with no agglomeration.

XPS analysis of the freshly prepared samples reveals Au in the metallic state and traces of sulphur due to the thiols used as stabilizers. After cleaning, the sulphur disappears, the ratio Au/C increases while the gold remains in the metallic state ($Au4f_{7/2}$ at 83.9-84.1 eV).

3.4. Ambient pressure photoelectron spectroscopy

In situ XPS experiments were performed with the gold nanoparticles supported over silica and titania thin films. Before the experiments, the samples were treated in oxygen (50 mtorr) at 130ºC to reduce the amount of hydrocarbons adsorbed on the surface. The oxygen was removed while the temperature was still high and the samples were allowed to cool in vacuum to ensure that no species were adsorbed on the surface.. Figure 9a and b shows the XPS spectra of the Au4f region of the 2 nm sample over SiO_2 and TiO_2 in vacuum (the results are similar for the 3.7 nm sample). When gold is supported on silicon oxide, metallic Au, with a binding energy of 84.1 eV, is exclusively observed. In the case of titania, two additional small contributions can be seen at 83.5 ($Au^{\delta-}$) and 85.3 eV ($Au^{\delta+}$). The $Au^{\delta-}$ species can originate from the interaction of gold with titanium. It is known that TiO_2 presents oxygen vacancies, with Ti^{3+} atoms in the lattice. Gold is more electronegative that titanium. Therefore, Ti can donate electron density to gold in order to compensate the oxygen vacancies, creating thus negatively charged gold species.

Under reaction conditions (130ºC, 0.1 torr of CO and 0.1 torr of O_2,) the Au4f peaks are shifted 0.3 eV to higher binding energies in both supports (TiO_2 and SiO_2). This shift could be due to the effect of the adsorbed CO, which withdraws electron density from the gold nanoparticles (Figure 9c and d). When the Au/SiO_2 samples were exposed to the reactant gases at room temperature, the XPS spectra did not change when compared to those acquired in vacuum, i.e., the gold atoms remain in the metallic state. However, for the Au/TiO_2 samples, there was a significant broadening of the XPS peaks corresponding to Au species.

The same experiment was performed with gold nanoparticles supported on powder TiO_2 (Figure 10). In vacuum the gold is in the metallic state and a 0.4 eV shift to higher binding energies is observed when exposed to reactant gases. Also, the gold peaks became broader in the presence of gases. The only work published until now using APPES with powder Au/TiO_2 catalysts prepared by deposition-precipitation also describes the shifting and broadening of the gold peaks (using Ti3p from the support as a reference). The authors attributed the shift and broadening to the oxidation of gold nanoparticles by the reactant gases [28]. Another possible explanation could be charging effects. This can be caused by charge transfer from the titanium to gold, which also transfers electron density to the antibonding states of the gases molecules [33]. This phenomenon could be the reason why titanium oxide support enhances the reactivity of Au in the CO oxidation [41], although more experimental evidence is needed to confirm these results.

4. Conclusions

Metallic gold nanoparticles prepared by colloidal chemistry with a sharp size distribution and deposited over SiO_2 (non reducible) and TiO_2 (reducible) supports were

used to elucidate the influence of the particle size and the support in the carbon monoxide oxidation reaction. Catalytic tests combined with characterization techniques demonstrate the key role of the particle size and the support in the reactivity of gold. On one hand, the activity increases as the gold particle size is decreased. On the other, the presence of a reducible support increases the activity when the temperature is higher than 50ºC. *In situ* ambient pressure photoelectron spectroscopy with powder and model planar samples (using the same nanoparticles) demonstrated that under reaction conditions the gold atoms remain in the metallic state with a slight shift to higher binding energies (~0.3-0.4 eV) due to the gases adsorbed. The promoting effect of the titanium dioxide could be due to the enhancement of the charge transfer between the gold and the antibonding states of the oxygen molecule, being activated in this way. However, more experimental evidence is necessary to clarify this point.

Acknowledgments

The work performed in the Advanced Light Source and the Molecular Foundry was supported by the Director, Office of Science, Office of Basic Energy Sciences, Chemical Sciences, Geosciences, and Biosciences Division, under the Department of Energy Contract No. DE-AC02-05CH11231. T.H. acknowledges also the financial support from the Ramon Areces Foundation.

References

1. B. Hammer, J.K. Nørskov, Nature 376 (1995) 238.

2 . M. Haruta, T. Kobayashi, H. Sano, N. Yamada, Chem. Lett., 2 (1987) 405.

3. M. Valden, X. Lai, D.W. Goodman, Science, 281 (1998) 1647.

4. M. Schubert, S. Hackenberg, A.C. van Veen, M. Muhler, V. Plzak, R.J. Behm, J. Catal., 197 (2001) 113.

5. M. Hatura, T. Tsubota , T. Kobayashi, H. Kageyama, M.J. Genet, B.J. Delmon, J. Catal, 144 (1993) 175.

6. A. Ueda, T. Ohshima and M. Haruta, Appl. Catal. B: Environ., 12 (1997) 81.

7. Catalysis by Gold, G.C. Bond, C. Louis, D. T. Thompson Eds., Catalytic Science Series-Vol 6 (2006) Imperial College Press, London.

8. S.H. Overbury, V. Schwartz, D.R. Mullins, W. Yana, S. Dai, J. Catal. 241 (2006) 56.

9. S. Arrii, F. Morfin, A. J. Renouprez, and J. L. Rousset J. Am. Chem. Soc., 126 (2004) 1199.

10. R.J.H. Grisel, B.E. Nieuwenhuys, J. Catal., 199 (2001) 48.

11. N. Lopez, T.V.W. Janssens, B.S. Clausen, Y. Xu, M. Mavrikakis, T. Bligaard, J.K. Nørskov, J. Catal., 223 (2004) 232.

12. M. Haruta, M. Daté, Appl. Catal. A:Gen., 222 (2001) 427.

13. I.N. Remediakis, N. Lopez, J.K. Norskov, Angew. Chem. Int. Ed., 44 (2005) 2.

14. G.C. Bond, D.T. Thompson, Gold, Bull., 33 (2000) 41.

15. M. Okumura, S. Nakamura, S. Tsuboata, T. Nakamura, M. Azuma, M. Haruta, Catal. Lett., 51 (1988) 53.

16. R.J. Davis, Science, 301 (2003) 926.

17. H. Häkkinen, S. Abbet, A. Sanchez, U. Heiz, U. Landman, Angew. Chem. Int. Ed., 42 (2003) 1297.

18. M.S. Chen, D.W. Goodman, Science, 306 (2004) 252.

19. B. Yoon, H. Häkkinen, U. Landman, A.S. Wörz, J.M. Antonietti, S. Abbet, K. Judai, U. Heiz, Science, 307 (2005) 403.

20. N. R. Jana and X. Peng, J. Am. Chem. Soc. 125 (2003) 14280.

21. N. Zheng, G.D. Stucky, J. Am. Chem. Soc., 128 (2006) 14278.

22. J.R. Heath, C. M. Knobler, D.V. Leff, J. Phys. Chem. B, 101 (1997) 197.

23. R.M. Rioux, H. Song, M. Grass, S. Habas, K. Niesz, J.D. Hoefelmeyer, P. Yang, G.A. Somorjai, Top. Catal., 39 (2006) 167.

24. E. L. Crepaldi, G. J.A.A. Soler-Illia, D.Grosso, F.Cagnol, F. Ribot, C.Sanchez, J. Am. Chem. Soc., 125 (2003) 9770.

25. P.C. Angelome, L. Andrini, M.E. Calvo, F.G. Requejo, S.A. Bilmes, G.J. A.A., Soler-Illia, J. Phys. Chem. C, 111 (2007) 10886.

26. D. F. Ogletree, H. Bluhm, G. Lebedev, C. S. Fadley, Z. Hussain and M. Salmeron, Rev. Sci. Inst., 73 (2002) 3872.

27. M. Salmeron, R. Schlogl, Surf. Sci. Rep., 63 (2008) 169.

28. E.A. Willneff, S. Braun, D. Rosenthal, H. Bluhm, M.l Hävecker, E. Kleimenov, A. Knop-Gericke, R. Schlögl, S. L. M. Schroeder, J. Am. Chem. Soc., 128 (2006) 12052.

29. S.H. Overbury, J. Catal. 241 (2006) 56.

30. M. Haruta, Stud. Surf. Sci. Catal. 110 (1997) 123.

31. M.M. Schubert, J.Catal., 197 (2001) 113.

32. Z.P. Liu, X.Q. Gong, J. Kohanoff, C. Sanchez, P.Hu, Physical Rev. Lett., 91 (2003) 266102.

33. Z.P. Liu, P. Hu, A. Alavi, J. Am. Chem. Soc., 124 (2002) 7499.

34. M. S. Pierce, K-C Chang, D. C. Hennessy, V. Komanicky, A. Menzel, H. You, J. Phys. Chem. C, *in press.*

35. X. Deng, B. K. min, A. Guloy, C. Friend, J. Am. Chem. Soc., 127 (2005) 9267.

36. L. Barrio, P. Liu, J.A. Rodriguez, J.M. Campos-Martin, J.L.G. Fierro, J. Phys. Chem. C. 111 (2007) 19001.

37. M. Mavrikakis, P. Stoltze, J.K. Norskov, Catal. Lett. 64 (2000) 101.

38. H. Falsig, B. Hvolbæk, I. S. Kristensen, T. Jiang, T. Bligaard, C. H. Christensen, J. K. Nørskov, Ang. Chem. Int. Ed., 47 (2008) 4835.

39. C. Louis, Gold nanoparticles: recent advances in CO oxidation in "Nanoparticles and Catalysis", Didier Astruc ed., Wiley-VCH (2008).

40. F. Bocuzzi, A. Chiorino, M. Manzoli, P. Lu, T. Akita, S. Ichikawa, M. Haruta, J. Catal., 202 (2001) 256.

41. J. A. Rodriguez, G. Liu, T. Jirsak, J. Hrbek, Z. Chang, J. Dvorak, A. Maiti, J. Am. Chem. Soc., 124 (2002) 5242.

6. Figure

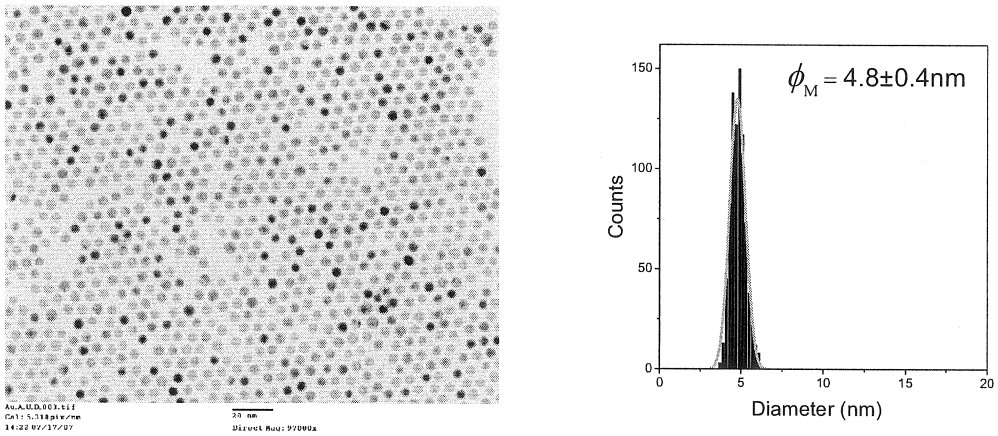

Figure 1. Transmisión electrón microscopy of 4.8 nm gold nanoparticles with particle size distribution.

6. Figure

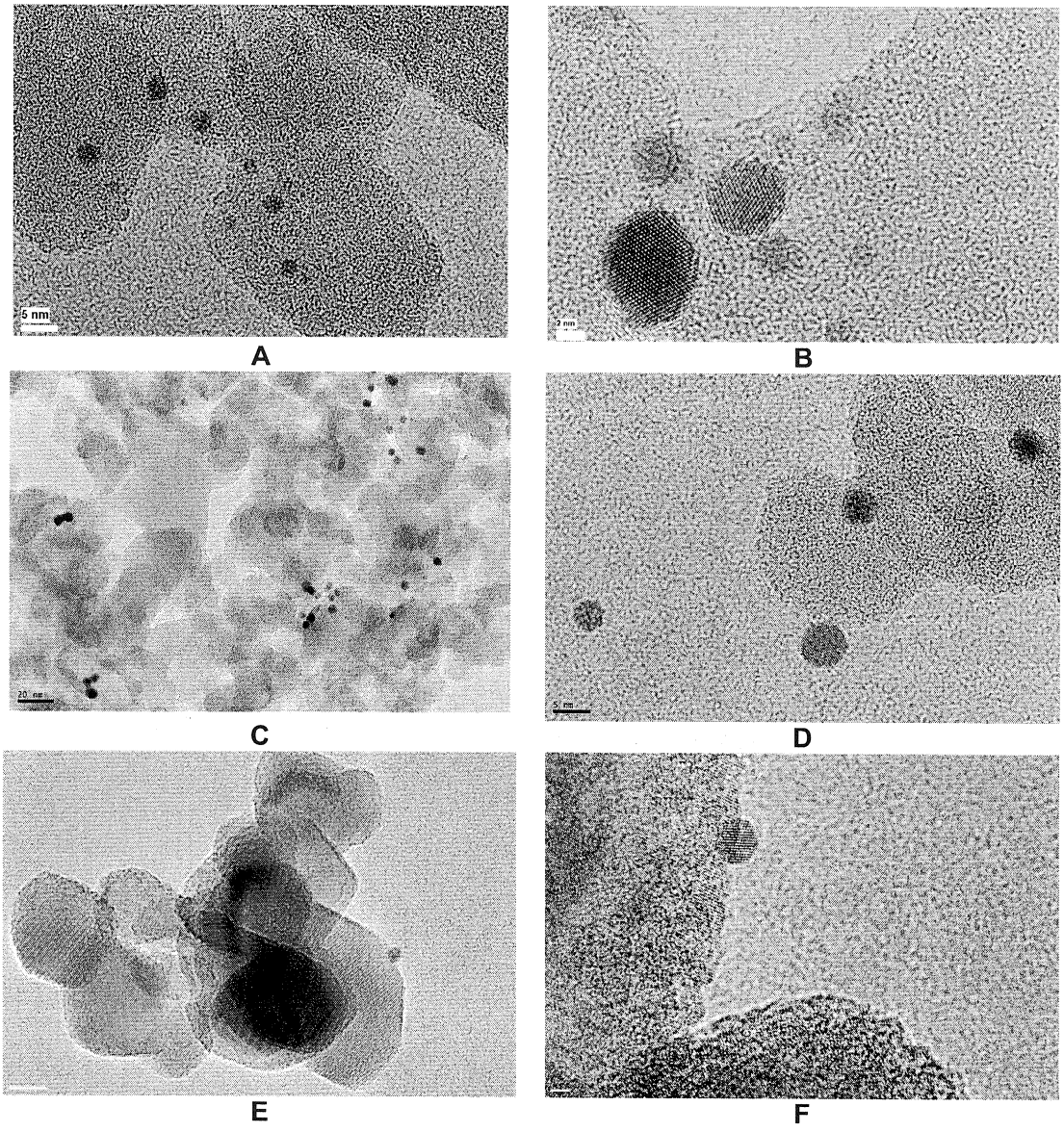

Figure 2. TEM and HRTEM micrographs of supported gold nanoparticles. a) and b) 2 nm supported over SiO_2. Size bars, 5 and 2 nm. c) and d) 3.7 nm over SiO_2. Size bars, 20 and 5 nm. e) and f) 4.1 nm over TiO_2. Size bars, 10 and 2 nm.

6. Figure

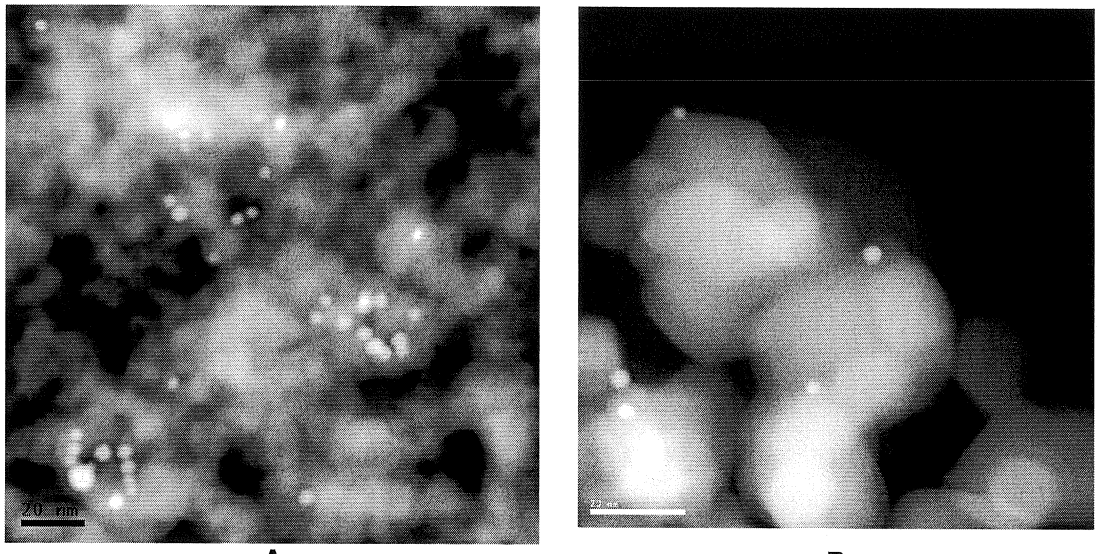

Figure 3. HAADF micrographs of a) 3.7 nm Au sample supported over SiO_2 (size bar 20 nm) and b) 2 nm sample supported over TiO_2 (size bar 20 nm).

6. Figure

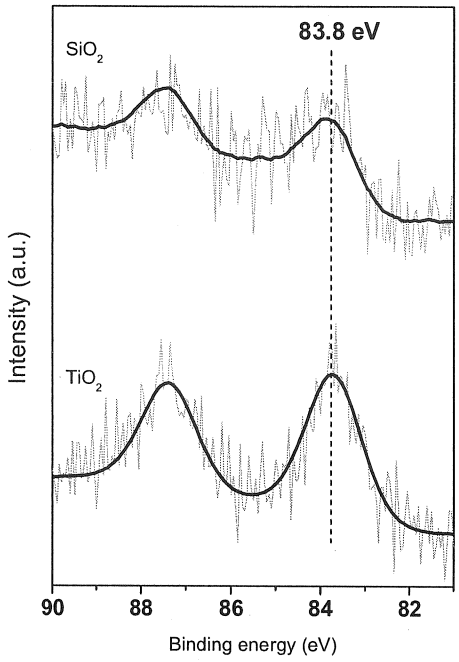

Figure 4. Au4f region of 2 nm nanoparticles supported over powder SiO_2 and TiO_2.

6. Figure

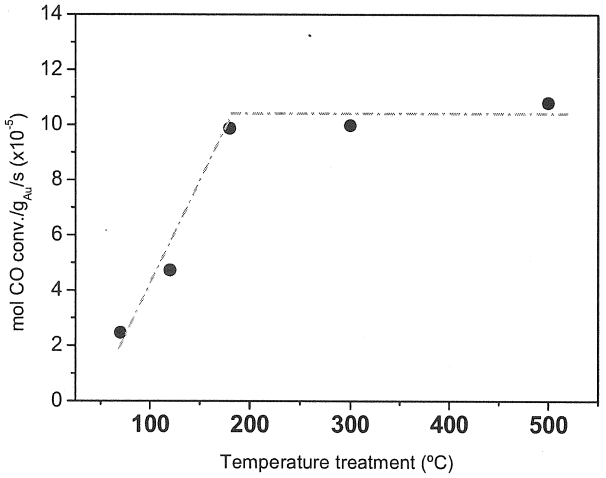

Figure 5. Specific activity (CO converted by gram of gold) of TiO_2 supported 2 nm nanoparticles in the CO oxidation reaction at 70ºC (gas flow 1CO:1O_2:4Ar, 30 ml/min total flow rate) versus the temperature of pretreatment in 10% O_2/Ar.

6. Figure

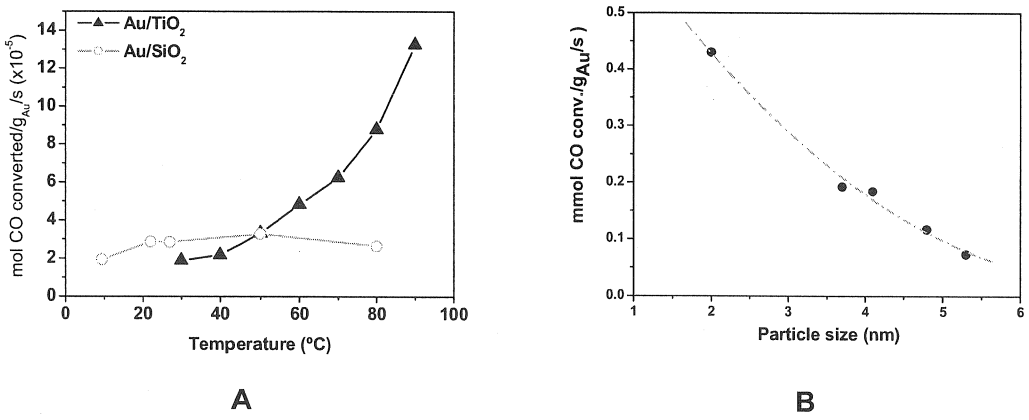

Figure 6. Catalytic activity (expressed as CO converted by gram of gold) of supported Au nanoparticles in the CO oxidation reaction (gas flow 1CO:1O_2:4Ar, 30 ml/min total flow rate). a) Effect of the support for the 3.7 nm particle size. b) Effect of the particle size for nanoparticles supported over TiO_2.

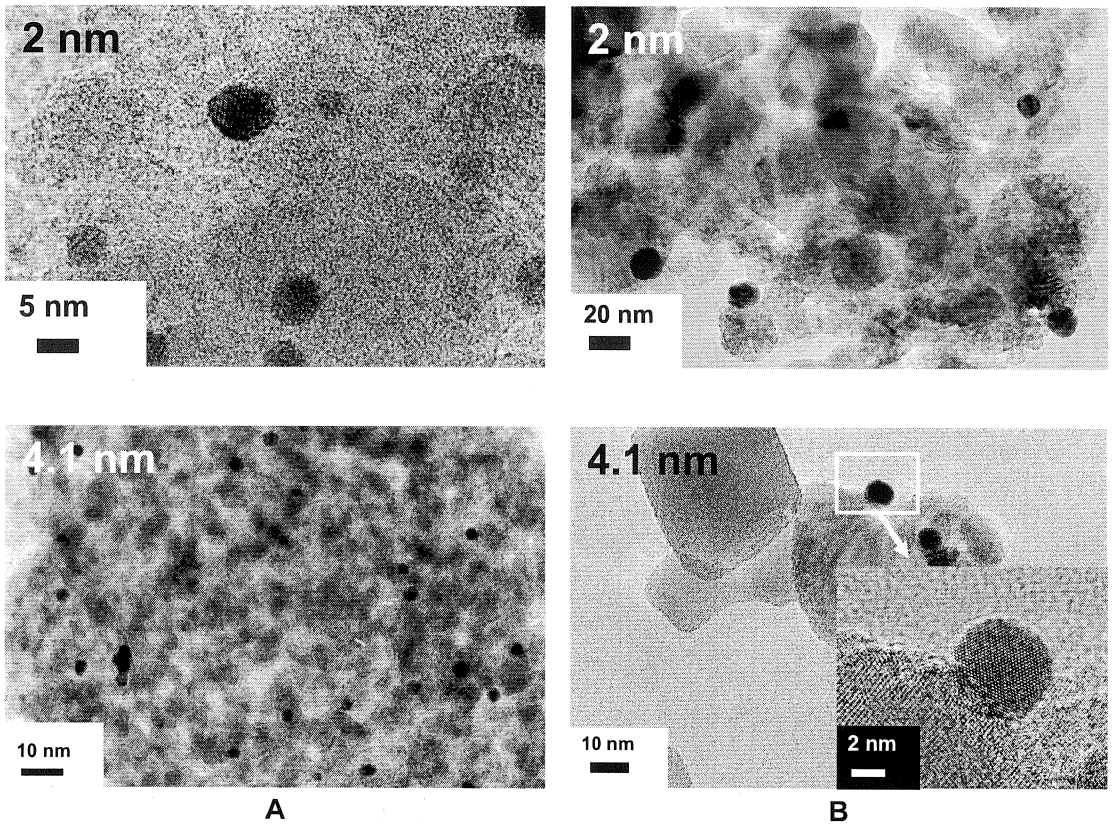

Figure 7. TEM micrographs of 2 and 4.1 nm supported gold nanoparticles after reaction. a) Samples supported over silicon oxide. b) Samples supported over titanium dioxide.

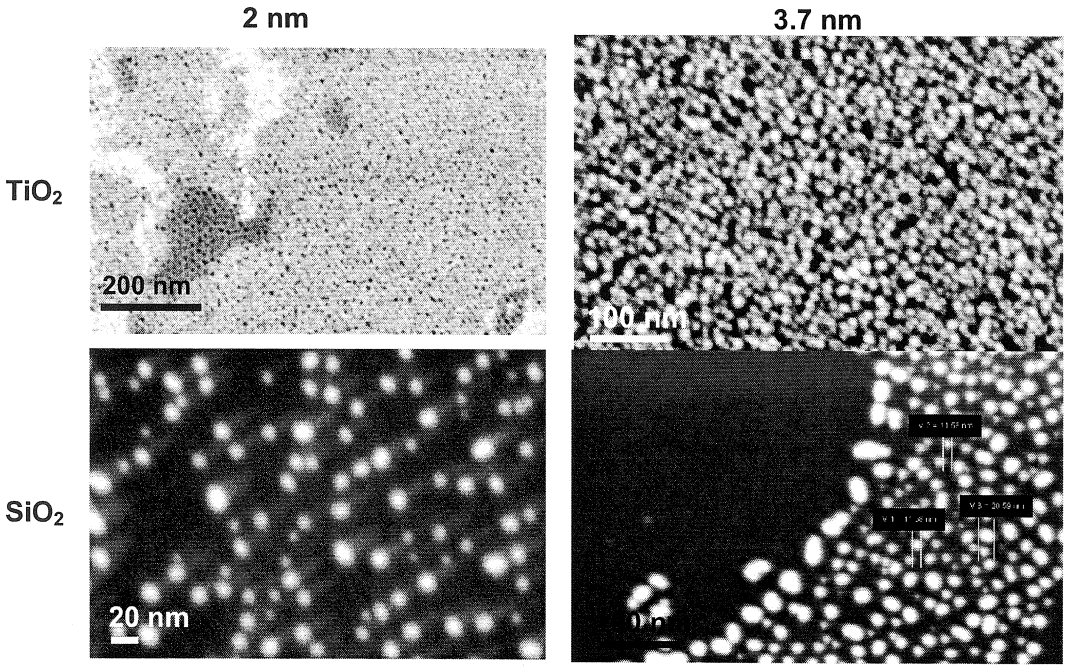

Figure 8. SEM micrographs of planar model catalysts prepared by Lagmuir-Blodgett using SiO_2 and TiO_2 thin films as supports and 2 and 3.7 nm gold nanoparticles. All the samples were cleaned with ozone for 60 min after preparation.

6. Figure

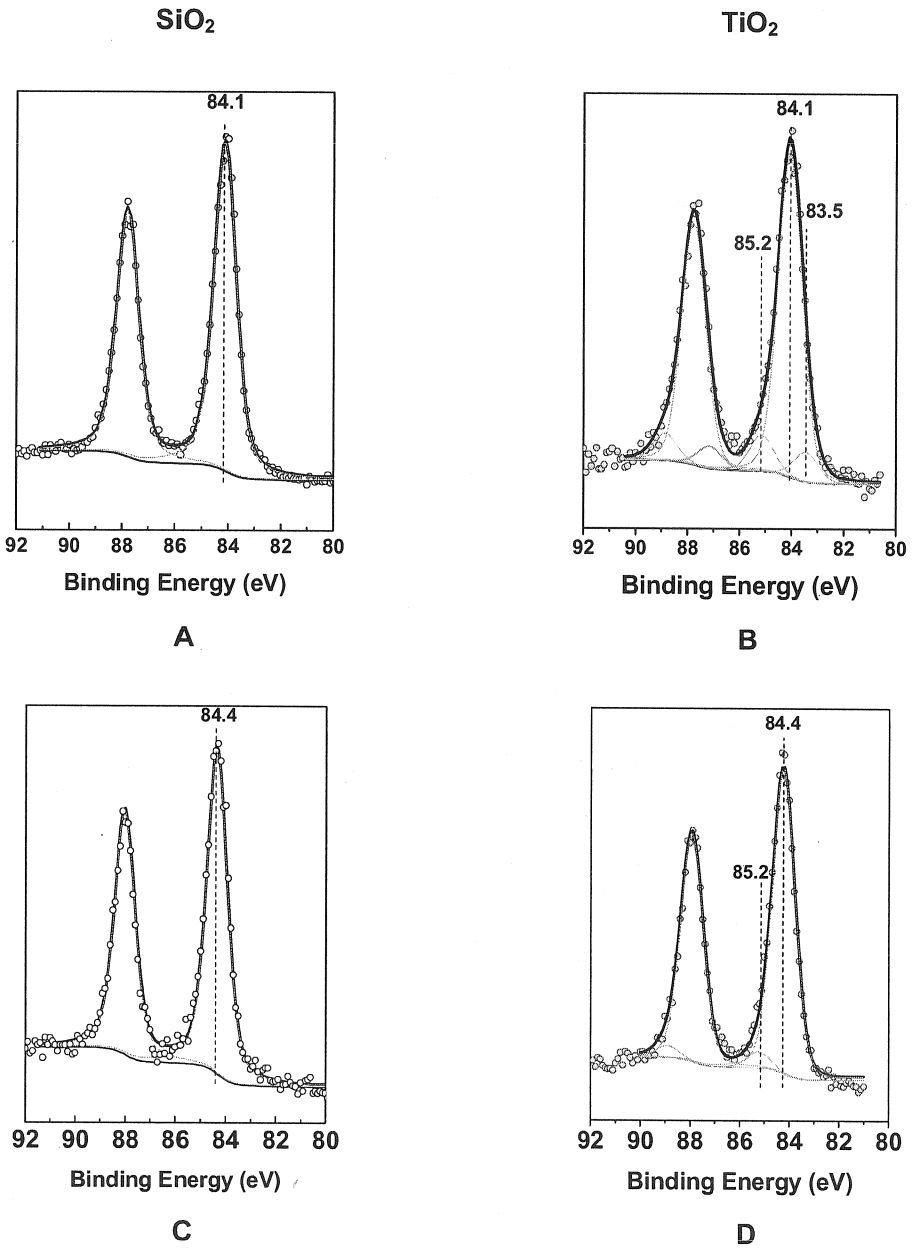

Figure 9. Au 4f region of 2 nm gold nanoparticles in planar samples measured by APPS in vacuum after cleaning with oxygen at 130ºC (a and b) and during reaction conditions: 150ºC and 0.1 torr of CO and O.1 torr of O_2 (c and d). a) and c) corresponds with SiO_2 support and b) and d) with TiO_2.

6. Figure

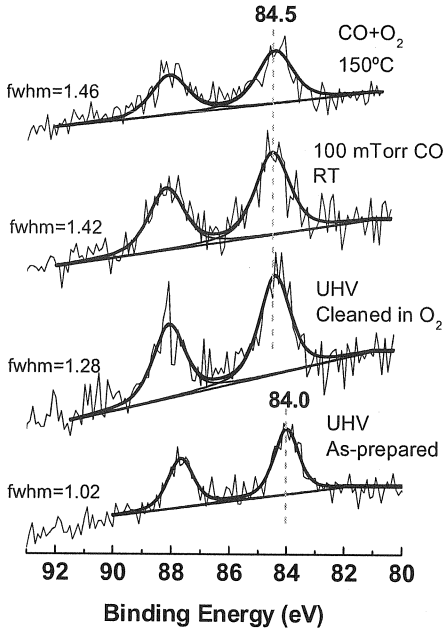

Figure 10. Au 4f region of 2 nm gold nanoparticles supported over powder titanium dioxide measured by APPS during exposure to CO (0.1 Torr) and reaction conditions (150ºC and 0.1 torr of CO and O.1 torr of O_2).